Ultra-thin mid-infrared silicon microring resonator

Qi He[1,2], Rongxiang Guo[1,2]*, Shujiao Zhang[1,2], Tiegen Liu[1,2], Zhenzhou Cheng[1,2,3]*

[1]*School of Precision Instruments and Optoelectronics Engineering, Tianjin University, Tianjin 300072, China*

[2]*Key Laboratory of Optoelectronics Information Technology, Ministry of Education, Tianjin 300072, China*

[3]*Georgia Tech-Shenzhen Institute, Tianjin University, Shenzhen 518055, China*

[*]*guorongxiang@tju.edu.cn; zhenzhoucheng@tju.edu.cn*

***Abstract*—A 70-nm thick mid-infrared silicon microring resonator with large evanescent-field energy of 83% is demonstrated. Experimental results show that the microring resonator has an extinction ratio of 16 dB and a Q factor of 2300 at the resonant wavelength of 2237 nm.**

Keywords—silicon photonics, mid-infrared, microring resonator

I. Introduction

Mid-infrared (mid-IR) silicon photonics exhibits great application potential for sensing and spectroscopy. In the mid-IR spectral range (2.0-20 μm), molecules have strong distinguishable absorption peaks due to the functional groups' strong stretching and bending vibrational transitions [1, 2]. Thus, molecules such as greenhouse gas molecules and biomolecules could be sensitively detected and accurately identified on mid-IR silicon chips [3, 4]. Besides, compared with the telecommunication band, mid-IR silicon waveguides have the advantage of lower optical scattering losses since the Rayleigh scattering intensity induced by the waveguide sidewall roughness is proportional to the inverse of the waveguide-guided light wavelength to the fourth power [5-7]. Therefore, mid-IR silicon photonic integrated circuits (PICs) are highly suitable for developing on-chip sensors and spectrometers.

Typically, the strength of the interaction between molecules and the electric field in silicon waveguides is essential in on-chip sensing applications [8]. As a type of widely used silicon photonic sensing device, namely, silicon microring resonators (MRRs), resonant wavelength shifts could be used for probing the environmental condition. While the sensitivity and limit of detection of the MRR-based sensors depend on the overlap between molecules and the optical mode fields of silicon waveguides. Consequently, many great efforts have been made to improve the evanescent-field ratio of the mid-IR silicon waveguide in the past decade, namely, slot waveguide [9], suspended waveguide [10, 11], and photonic crystal waveguide [12]. However, previous mid-IR silicon devices with a top silicon layer thickness of several hundred nanometers still have moderate evanescent-field ratios.

Here, we demonstrated a 70-nm thick mid-IR silicon MRR. By reducing the top silicon thickness and removing the buried oxide (BOX) of the devices, the evanescent-field ratio of the developed MRRs has been greatly improved. The devices were fabricated based on a standard multi-project wafer (MPW) service, while the BOX was removed by using a post-fabrication process, namely, immersing the fabricated chip in a dilute hydrofluoric acid solution. The ultra-thin MRR has a large evanescent-field ratio of 83% with an extinction ratio of 16 dB and a Q factor of 2300 at a resonance wavelength of 2237 nm. Our results pave the potential way for developing mid-IR on-chip molecular sensors for applications of medical diagnosis, environmental monitoring, and industrial safety.

II. Design of the Mid-IR Ultra-Thin Silicon MRR

As shown in Fig. 1(a), ultra-thin mid-IR devices were designed based on a commercially available silicon-on-insulator (SOI) wafer which has a top-layer silicon thickness of 220 nm and a BOX thickness of 3 μm. Ultra-thin subwavelength grating (SWG) couplers [13] were designed to couple the light into/out of the ultra-thin silicon waveguide, while a bus waveguide connecting with the grating couplers was designed to couple the light into the MRR. Besides, the radius of the MRR was designed as 60 μm while the gap between the bus waveguide and MRR was set as 300 nm to achieve the critical coupling of the MRR. To increase the devices' evanescent-field energy in the air, the thickness of the devices was reduced to 70 nm while the BOX below the silicon waveguide was designed to remove. Moreover, the removal of the BOX could reduce the optical absorption loss of the silica to the mid-IR light. To strengthen the mechanical stability, the ultra-thin bus waveguide and the ultra-thin MRR were designed to be supported by the SWG cladding, as shown in Fig. 1(b). And the fundamental transverse electric mode (TE_0) of the suspended SWG-cladding ultra-thin silicon waveguide could be supported. As the thickness of the top silicon layer decreases from 220 nm to 70 nm, a giant energy ratio of the TE_0 mode is located in the air as the evanescent field, and the evanescent-field ratio could increase to 83% theoretically which is about three times larger than that of the 220-nm thick silicon waveguide.

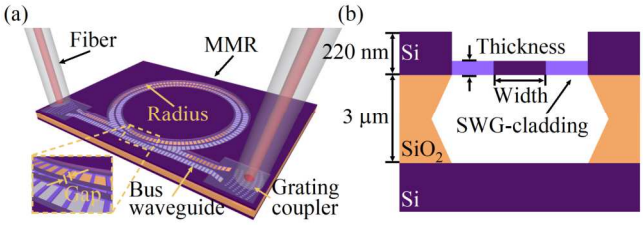

Fig. 1. Schematic and simulation of the mid-IR ultra-thin silicon MRR. (a) Schematic of the ultra-thin MRR in the 3D view. (b) Schematic of the SWG-cladding waveguide in the cross-section view.

III. Fabrication and Characterization

The devices were fabricated based on an MPW service followed by a wet-etching process. In the MPW service, a 180-nm CMOS-process line was used to pattern an SOI wafer with three etch depths of 70 nm, 150 nm, and 220 nm, respectively. Firstly, the silicon wafer was etched with a depth of 150 nm remaining a 70 nm thick silicon layer. Then, devices were fabricated on the remaining silicon region. After the MPW fabrication, the fabricated chip was immersed in a 7.6% dilute hydrofluoric acid solution for 90 minutes to remove the BOX under the devices. Fig. 2 shows the scanning electron microscope (SEM) images of the fabricated devices. In the top view of the device, as shown in Fig. 2(a), SWG couplers, bus waveguide, and MRR were fabricated with sizes that matched well with our design. Besides, the BOX under the device was locally removed while the ultra-thin devices were suspended in the air without collapsing or breakings. In

the zoom-in view of the coupling area of the MRR, as shown in Fig. 2(b), the gap between the bus waveguide and MRR with a width of several nanometers could be clearly observed.

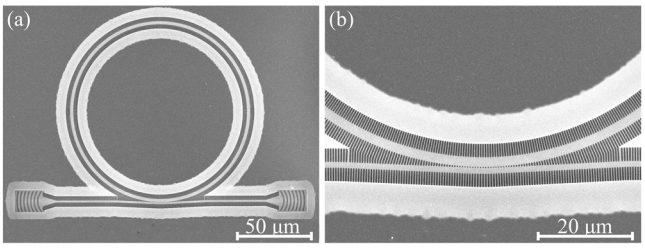

Fig. 2. SEM images of the mid-IR ultra-thin MRR and ultra-thin SWG coupler. (a) Top view of the device. (b) Zoom-in view of the coupling area between the ultra-thin bus waveguide and ultra-thin MRR.

In the device measurement, we characterized the mid-IR ultra-thin silicon MRR by using an experimental system consisting of a continuous-wave Cr^{2+}:ZnS/Se tunable laser, InGaAs photodiode power meter, fiber alignment system, and Ge-doped silica-core optical fiber. Firstly, we measured the transmission spectrum of the ultra-thin device with a spectral range covering from 2210 nm to 2300 nm wavelengths. Then, we used the coupling efficiency curve of the SWG coupler to normalize the transmission spectrum of the device to obtain the transmission spectrum of the ultra-thin silicon MRR, as shown in Fig. 3(a). It can be observed that the ultra-thin silicon MRR has eleven resonances in this spectral range with a free space range (FSR) of 8.8 nm. Furthermore, we measured the FSR of the ultra-thin MRR with radii of 20 μm, 40 μm, 80 μm, and 100 μm, respectively. As shown in Fig. 3(b), the FSR of the ultra-thin MRR increases as the reciprocal of the radius increases. After the linear fitting of the measurement results, the group refractive index (n_g = 1.68) of the ultra-thin MRR could be calculated through the equation of $n_g=\lambda^2/(2\pi R\cdot FSR)$, where the λ is the resonance wavelength of the ultra-thin silicon MRR. Finally, the transmission spectrum of the ultra-thin MRR at the resonance wavelength of 2337 nm was measured. As shown in Fig. 3(c), the ultra-thin MRR has a large extinction ratio (ER) of 16 dB and a linewidth of 0.98 nm corresponding to a Q factor of ~2300.

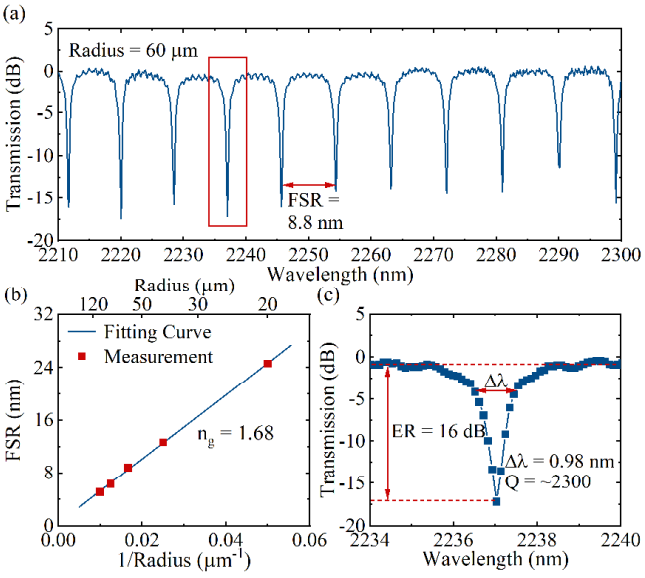

Fig. 3. Experimental results of the mid-IR ultra-thin silicon MRR. (a) Transmission spectrum of the ultra-thin MRR with the radius of 60 μm. (b) FSR of the ultra-thin MRR with the radius of 20 μm, 40 μm, 60 μm, 80 μm, and 100 μm. (c) Zoom-in spectrum of the MRR transmission at the resonance wavelength of 2237 nm.

IV. Conclusion

In conclusion, we demonstrated a mid-IR ultra-thin MRR with a giant evanescent-field ratio. By reducing the thickness of the top silicon layer of the MRR from 220 nm to 70 nm, the evanescent-field ratio could increase from 30% to 83%. The ultra-thin MRR has a large FSR of 8.8 nm corresponding to a small n_g of 1.68. Besides, the fine transmission spectrum shows that the ultra-thin MRR has an ER of 16 dB and a linewidth of 0.98 nm corresponding to a Q factor of ~2300. Our study opens a promising avenue for developing ultra-thin mid-IR silicon PICs for on-chip sensing and spectroscopy applications.

Acknowledgment

The work was partly supported by the National Natural Science Foundation of China (62175179, 62161160335), and the National Natural Science Foundation of Guangdong Province (2022B1515130002).

References

[1] Schliesser, Albert; Picqué, Nathalie; and Hänsch, Theodor W.; Mid-infrared frequency combs, Nature Photonics, 2012, 6(7), 440-449.

[2] Muraviev, A. V.; Smolski, V. O.; Loparo, Z. E.; and Vodopyanov, K. L.; Massively parallel sensing of trace molecules and their isotopologues with broadband subharmonic mid-infrared frequency combs, Nature Photonics, 2018, 12(4), 209-214.

[3] Zou, Yi; Chakravarty, Swapnajit; Wray, Parker; and Chen, Ray T.; Mid-infrared holey and slotted photonic crystal waveguides in silicon-on-sapphire for chemical warfare simulant detection, Sensors and Actuators B: Chemical, 2015, 221, 1094-1103.

[4] Grassani, Davide; Tagkoudi, Eirini; Guo, Hairun; Herkommer, Clemens; Yang, Fan; Kippenberg, Tobias J.; and Brès, Camille-Sophie; Mid infrared gas spectroscopy using efficient fiber laser driven photonic chip-based supercontinuum, Nature Communications, 2019, 10(1), 1553.

[5] Xia, Xin; Chen, Qi; Tsay, Candice; Arnold, Craig B.; and Madsen, Christi K.; Low-loss chalcogenide waveguides on lithium niobate for the mid-infrared, Optics Letters, 2010, 35(19), 3228-3230.

[6] Guo, Rongxiang; Zhang, Shujiao; Gao, Haoran; Senthil Murugan, Ganapathy; Liu, Tiegen; and Cheng, Zhenzhou; Blazed subwavelength grating coupler, Photonics Research, 2023, 11(2), 189-195.

[7] Chen, Weicheng; Wu, Jingwen; Wan, Dian; Wang, Jie; Wang, Jiaqi; Zou, Yi; Cheng, Zhenzhou; and Liu, Tiegen; Grating couplers beyond silicon TPA wavelengths based on MPW, Journal of Physics D: Applied Physics, 2021, 55(1).

[8] Vlk, Marek; Datta, Anurup; Alberti, Sebastián; Yallew, Henock Demessie; Mittal, Vinita; Murugan, Ganapathy Senthil; and Jágerská, Jana; Extraordinary evanescent field confinement waveguide sensor for mid-infrared trace gas spectroscopy, Light: Science & Applications, 2021, 10(1), 26.

[9] Penadés, J. S.; Khokhar, A. Z.; Nedeljkovic, M.; and Mashanovich, G. Z.; Low-Loss Mid-Infrared SOI Slot Waveguides, IEEE Photonics Technology Letters, 2015, 27(11), 1197-1199.

[10] Soler Penadés, J.; Alonso-Ramos, C.; Khokhar, A. Z.; Nedeljkovic, M.; Boodhoo, L. A.; Ortega-Moñux, A.; Molina-Fernández, I.; Cheben, P.; and Mashanovich, G. Z.; Suspended SOI waveguide with sub-wavelength grating cladding for mid-infrared, Optics Letters, 2014, 39(19), 5661-5664.

[11] Cheng, Z.; Chen, X.; Wong, C. Y.; Xu, K.; and Tsang, H. K.; Mid-infrared Suspended Membrane Waveguide and Ring Resonator on Silicon-on-Insulator, IEEE Photonics Journal, 2012, 4(5), 1510-1519.

[12] Reimer, Christian; Nedeljkovic, Milos; Stothard, David J. M.; Esnault, Matthieu O. S.; Reardon, Christopher; O'Faolain, Liam; Dunn, Malcolm; Mashanovich, Goran Z.; and Krauss, Thomas F.; Mid-infrared photonic crystal waveguides in silicon, Optics Express, 2012, 20(28), 29361-29368.

[13] Guo, Rongxiang; Gao, Haoran; Liu, Tiegen; and Cheng, Zhenzhou; Ultra-thin mid-infrared silicon grating coupler, Optics Letters, 2022, 47(5), 1226-1229.